

# Verification-Friendly Deep Neural Networks

Anahita Baninajjar

*Electrical and Information Technology*  
Lund University  
Lund, Sweden  
anahita.baninajjar@eit.lth.se

Ahmed Rezine

*Computer and Information Science*  
Linköping University  
Linköping, Sweden  
ahmed.rezine@liu.se

Amir Aminifar

*Electrical and Information Technology*  
Lund University  
Lund, Sweden  
amir.aminifar@eit.lth.se

**Abstract**—Machine learning techniques often lack formal correctness guarantees. This is evidenced by the widespread adversarial examples that plague most deep-learning applications. This resulted in several research efforts that aim at verifying deep neural networks, with a particular focus on safety-critical applications. However, formal verification techniques still face major scalability and precision challenges when dealing with the complexity of such networks. The over-approximation introduced during the formal verification process to tackle the scalability challenge often results in inconclusive analysis. To address this challenge, we propose a novel framework to generate Verification-friendly Neural Networks (VNNs). We present a post-training optimization framework to achieve a balance between preserving prediction performance and robustness in the resulting networks. Our proposed framework proves to result in networks that are comparable to the original ones in terms of prediction performance, while amenable to verification. This essentially enables us to establish robustness for more VNNs than their deep neural network counterparts, in a more time-efficient manner.

**Index Terms**—neural networks, formal verification, adversarial examples, robustness

## I. INTRODUCTION

The state-of-the-art machine learning techniques often lack formal correctness guarantees. This has been demonstrated by a wide range of “adversarial examples” in the deep learning domain [1, 2, 3] and presents a major challenge in the context of safety-critical applications [4]. To address this challenge, several robustness verification frameworks for Deep Neural Networks (DNNs) have been proposed in the state of the art [5, 6, 7, 8]. However, the overwhelming majority of the state-of-the-art verification techniques suffer from poor scalability. As a result, the main body of work in state-of-the-art aims to improve the scalability of the existing robustness verification frameworks for DNNs [9, 10, 11].

In contrast to this majority of the state-of-the-art verification techniques, here in this paper, we propose a new generation of DNNs that are amenable to verification, or simply verification friendly. Verification-friendly Neural Networks (VNNs) allow more efficiency, in terms of time, and/or more verified samples, while maintaining on-par performance with their DNN counterparts. The key observation is that the majority of the robustness verification frameworks are based on over-approximation

and this over-approximation accumulates/amplifies along the forward pass. To reduce this over-approximation, we formulate this problem as an optimization and enforce sparsity on the DNNs to obtain VNNs, allowing verification tools to establish robustness.

We evaluate our proposed approach based on the classical MNIST image dataset [12] and demonstrate that VNNs are indeed amenable to verification, while maintaining the same prediction performance as their DNN counterparts. The time required for verification is always less than that of the original models (up to 50% in some cases) due to the sparsity of the VNNs. At the same time, and more importantly, we observe that VNNs allow verification of up to 140 times more samples, besides their advantage in terms of verification time efficiency.

In addition to the MNIST image dataset, to evaluate our work on real-world safety-critical applications, we consider two datasets from the medical domain, i.e., real-time epileptic seizure detection based on the electroencephalogram (EEG) data in CHB-MIT dataset [13] and real-time cardiac arrhythmia detection based on the electrocardiogram (ECG) data in MIT-BIH dataset [14]. Failure to detect an epileptic seizure or a cardiac arrhythmia episode in time may have irreversible consequences and potentially lead to death [15, 16]. For such safety-critical applications, we demonstrate that the number of verified samples with VNNs is up to 25 times more than DNNs, considering the CHB-MIT and MIT-BIH datasets. We also demonstrate that our proposed framework is substantially more effective than straightforward sparsifying/pruning that does not consider the already-existing patterns captured by the DNNs.

## II. VERIFICATION-FRIENDLY NEURAL NETWORKS

In this section, we discuss our proposed framework to generate Verification-friendly Neural Network (VNN) models. The framework comes with an optimization problem that takes a trained model as input (i.e., the original network) and that results in a VNN model. We will introduce the optimization problem, explain the formulation of the objective function and constraints, and describe their relaxations.

### A. Deep Neural Networks

Let us first formalize our notation for DNNs. A neural network is a series of linear transformations and nonlinear

This research has been partially supported by the Swedish Wallenberg AI, Autonomous Systems and Software Program (WASP), the Swedish Research Council (VR), and the European Union (EU) Interreg Program.

activation functions to generate outputs using trained weights and biases. We consider  $f_k(\cdot) : R^{n_{k-1}} \rightarrow R^{n_k}$  as a function that generates values of the  $k$ th layer from its previous layer, where  $n_k$  shows the number of neurons in the  $k$ th layer. Then, the values of the  $k$ th layer,  $\mathbf{x}^{(k)}$ , are given by  $\mathbf{x}^{(k)} = f_k(\mathbf{x}^{(k-1)}) = \text{act}(\mathbf{W}^{(k)}\mathbf{x}^{(k-1)} + \mathbf{b}^{(k)})$ , such that  $\mathbf{W}^{(k)}$  and  $\mathbf{b}^{(k)}$  are the weights and biases of the  $k$ th layer and  $\text{act}$  is the activation function.

### B. Layer-Wise Optimization Problem

To obtain VNNs, our aim is to minimize the number of non-zero weights  $\tilde{\mathbf{W}}^{(l)}$  and biases  $\tilde{\mathbf{b}}^{(l)}$  of the  $l$ th layer of an  $N$ -layer neural network to have a model that is more sparse while still accurate. In the following, we outline our proposed optimization problem to obtain VNNs:

$$\min_{\tilde{\mathbf{W}}^{(l)}, \tilde{\mathbf{b}}^{(l)}} \|\tilde{\mathbf{W}}^{(l)}\|_{0,0} + \|\tilde{\mathbf{b}}^{(l)}\|_0, \quad (1)$$

$$\text{s.t. } \mathbf{x}^{(k)} = f_k(\mathbf{x}^{(k-1)}), \forall k \in \{1, \dots, N\} \quad (2)$$

$$\tilde{\mathbf{x}}^{(l)} = \tilde{f}_l(\mathbf{x}^{(l-1)}), \quad (3)$$

$$\tilde{\mathbf{x}}^{(m)} = f_m(\tilde{\mathbf{x}}^{(m-1)}), \forall m \in \{l+1, \dots, N\}, \quad (4)$$

$$\|\tilde{\mathbf{x}}^{(l)} - \mathbf{x}^{(l)}\|_\infty \leq \epsilon, \quad (5)$$

$$\arg \max \mathbf{x}^{(N)} = \arg \max \tilde{\mathbf{x}}^{(N)} = y, \quad (6)$$

$$\forall \mathbf{x}^{(0)} \in \mathbf{D}_{val}. \quad (7)$$

To minimize the number of non-zero weights  $\tilde{\mathbf{W}}^{(l)}$  and biases  $\tilde{\mathbf{b}}^{(l)}$ , we consider the  $L_0$  norm  $\|\cdot\|_0$ , also known as the sparse norm, as the objective function. The  $L_0$  norm counts the number of non-zero elements in a vector or matrix. Therefore, the objective function is  $\|\tilde{\mathbf{W}}^{(l)}\|_{0,0} + \|\tilde{\mathbf{b}}^{(l)}\|_0$  to find the minimum number of non-zero elements in  $\tilde{\mathbf{W}}^{(l)}$  and  $\tilde{\mathbf{b}}^{(l)}$ , as shown in Equation (1).

Let us consider the constraints in Equations (2)–(7). Equation (2) establishes the original values of the neural network with the trained weights and biases. For setting up the neurons' values after optimization, we define  $\tilde{f}_l(\cdot) : R^{n_{l-1}} \rightarrow R^{n_l}$  as the new nonlinear function that transfers values of the  $(l-1)$ th layer to the target layer  $l$  using the optimized weights and biases. Therefore,  $\tilde{\mathbf{x}}^{(l)}$  is given by  $\tilde{\mathbf{x}}^{(l)} = \tilde{f}_l(\mathbf{x}^{(l-1)}) = \text{act}(\tilde{\mathbf{W}}^{(l)}\mathbf{x}^{(l-1)} + \tilde{\mathbf{b}}^{(l)})$  in Equation (3). The change of neurons' values in layer  $l$  may result in different values for the neurons of the next layer, hence we introduce Equation (4). Equation (5) ensures that  $\tilde{\mathbf{x}}^{(l)}$  takes a value within the neighborhood of  $\epsilon$  around  $\mathbf{x}^{(l)}$  to avoid extreme changes. In Equation (6), the optimization problem is constrained to keep the same class as the one derived by the neural network prior to the optimization. Consider that the input  $\mathbf{x}^{(0)}$  belongs to class  $c$ . This means  $\mathbf{x}_c^{(N)} > \mathbf{x}_i^{(N)}$  for all neurons  $i \neq c$  in the last layer. To obtain the same class after optimization, the same has to hold for  $\tilde{\mathbf{x}}_i^{(N)}$ , i.e.,  $\tilde{\mathbf{x}}_c^{(N)} > \tilde{\mathbf{x}}_i^{(N)}$  for all neurons  $i \neq c$  in the last layer, which can be formulated in the context of our linear optimization problem. However, for the simplicity of the presentation, we adopt the compact form

of this constraint in Equation (6) in the remainder of this paper. In Equation (6),  $y$  is the label of each  $\mathbf{x}^{(0)}$  in the validation set  $\mathbf{D}_{val}$ . All constraints need to hold for all inputs in the validation set  $\mathbf{D}_{val}$  (Equation (7)). We consider the validation set instead of the training one to avoid over-fitting weights and biases.

### C. Relaxation of Objective Function

Optimizing the  $L_0$  norm poses significant challenges due to the non-convex nature of the  $L_0$  norm. Here, we will elaborate on how to overcome this difficulty. The  $L_0$  norm is expressed in the form of an  $L_p$  norm, but to be precise, it is not actually a norm [17]. As mentioned in the previous section, The problem with using the  $L_0$  norm is its non-convexity.

The  $L_1$  norm also referred to as the Manhattan norm, is the tightest convex relaxation of the  $L_0$  norm in convex optimization [18]. While the  $L_0$  norm counts the number of non-zero elements of a matrix, the  $L_1$  norm sums the absolute values of the elements. Being a convex function, the  $L_1$  norm can be used in convex optimization problems, which is not possible with the  $L_0$  norm. Therefore, the optimization objective is reformulated as follows to be convex:

$$\min_{\tilde{\mathbf{W}}^{(l)}, \tilde{\mathbf{b}}^{(l)}} \|\tilde{\mathbf{W}}^{(l)}\|_{1,1} + \|\tilde{\mathbf{b}}^{(l)}\|_1. \quad (8)$$

### D. Relaxation of Constraints

The constraints of the optimization problem are nonlinear, and the nonlinearity is caused by the activation functions in  $f_k(\cdot)$  and  $\tilde{f}_l(\cdot)$ . Henceforth, we perform the analysis on the ReLU activation function, which is the most popular activation function in neural networks, but our framework can be extended to any nonlinear activation function that can be presented in a piece-wise linear form.

Performing function  $\text{ReLU}(x) = \max(0, x)$  results in two possible states for each neuron  $x_i^{(l)}$ . Suppose  $f_{l,i}(\cdot)$  performs  $f_l(\cdot)$  for neuron  $x_i^{(l)}$ ; The neuron either remains continuously active if  $f_{l,i}(\mathbf{x}^{(l-1)}) = \mathbf{W}_{i,:}^{(l)}\mathbf{x}^{(l-1)} + b_i^{(l)} > 0$ , or becomes permanently inactive when  $f_{l,i}(\mathbf{x}^{(l-1)}) = 0$  or  $\mathbf{W}_{i,:}^{(l)}\mathbf{x}^{(l-1)} + b_i^{(l)} \leq 0$ . This reflects that the ReLU function is a combination of linear segments, creating a piece-wise linear function. If we constrain the neuron to remain within one of these linear segments, the ReLU function behaves linearly, making it possible to handle the proposed optimization. Therefore, the neurons in the target layer  $l$  must remain in the same state (or in the same linear segment). This is formulated as follows for  $\tilde{x}_i^{(l)}$ :

$$\begin{cases} \tilde{\mathbf{W}}_{i,:}^{(l)}\mathbf{x}^{(l-1)} + \tilde{b}_i^{(l)} \geq 0 & \text{if } f_{l,i}(\mathbf{x}^{(l-1)}) > 0, \\ \tilde{\mathbf{W}}_{i,:}^{(l)}\mathbf{x}^{(l-1)} + \tilde{b}_i^{(l)} \leq 0 & \text{otherwise.} \end{cases} \quad (9)$$

The above introduces a new constraint for each neuron  $i$ , where if the neuron has been originally active ( $f_{l,i}(\mathbf{x}^{(l-1)}) = \mathbf{W}_{i,:}^{(l)}\mathbf{x}^{(l-1)} + b_i^{(l)} > 0$ ), we constrain the new weights and bias to also remain active ( $\tilde{\mathbf{W}}_{i,:}^{(l)}\mathbf{x}^{(l-1)} + \tilde{b}_i^{(l)} \geq 0$ ); otherwise (if the neuron has originally been inactive, i.e.,  $f_{l,i}(\mathbf{x}^{(l-1)}) = 0$

or  $\mathbf{W}_{i,:}^{(l)} \mathbf{x}^{(l-1)} + b_i^{(l)} \leq 0$ , we constrain the new weights and bias to also remain inactive ( $\tilde{\mathbf{W}}_{i,:}^{(l)} \mathbf{x}^{(l-1)} + \tilde{b}_i^{(l)} \leq 0$ ).

In this framework, the values of the neurons in layers  $k < l$  remain unchanged during the optimization process, but the output of layer  $l$  will change. Changing neurons' values of layer  $l$  may cause an alteration in the values of any neuron of the following layers  $m > l$ , which could potentially influence the classification result. To guarantee the consistency of the class assigned to each sample, we have to capture the whole neural network. To do so, we once more leverage on the piecewise linearity of the ReLU function. Suppose  $f_{m,i}(\cdot)$  performs  $f_m(\cdot)$  for neuron  $x_i^{(m)}$ . We formulate neuron  $x_i^{(m)}$  in layer  $m > l$  as follows:

$$\begin{cases} \mathbf{W}_{i,:}^{(m)} \mathbf{x}^{(m-1)} + b_i^{(m)} \geq 0 & \text{if } f_{m,i}(\mathbf{x}^{(m-1)}) > 0, \\ \mathbf{W}_{i,:}^{(m)} \mathbf{x}^{(m-1)} + b_i^{(m)} \leq 0 & \text{otherwise.} \end{cases} \quad (10)$$

### E. Relaxation of Layer-Wise Optimization Problem

After relaxing the objective function and the constraints, we state in the following our proposed layer-wise optimization problem as a linear program:

$$\begin{aligned} & \min_{\tilde{\mathbf{W}}^{(l)}, \tilde{\mathbf{b}}^{(l)}} \|\tilde{\mathbf{W}}^{(l)}\|_{1,1} + \|\tilde{\mathbf{b}}^{(l)}\|_1, \\ & \text{subject to:} \\ & \mathbf{x}^{(k)} = f_k(\mathbf{x}^{(k-1)}), \forall k \in \{1, \dots, N\} \\ & \begin{cases} \tilde{x}_i^{(l)} = \tilde{\mathbf{W}}_{i,:}^{(l)} \mathbf{x}^{(l-1)} + \tilde{b}_i^{(l)} \geq 0 & \text{if } f_{l,i}(\mathbf{x}^{(l-1)}) > 0, \\ \tilde{x}_i^{(l)} = 0, \tilde{\mathbf{W}}_{i,:}^{(l)} \mathbf{x}^{(l-1)} + \tilde{b}_i^{(l)} \leq 0 & \text{otherwise} \end{cases} \\ & \forall j \in \{1, \dots, n_l\}, \\ & \begin{cases} \tilde{x}_j^{(m)} = \mathbf{W}_{j,:}^{(m)} \tilde{\mathbf{x}}^{(m-1)} + b_j^{(m)} \geq 0 & \text{if } f_{m,j}(\tilde{\mathbf{x}}^{(m-1)}) > 0, \\ \tilde{x}_j^{(m)} = 0, \mathbf{W}_{j,:}^{(m)} \tilde{\mathbf{x}}^{(m-1)} + b_j^{(m)} \leq 0 & \text{otherwise} \end{cases} \\ & \forall j \in \{1, \dots, n_m\}, \forall m \in \{l+1, \dots, N\}, \\ & \|\tilde{\mathbf{x}}^{(l)} - \mathbf{x}^{(l)}\|_\infty \leq \epsilon, \\ & \arg \max \mathbf{x}^{(N)} = \arg \max \tilde{\mathbf{x}}^{(N)} = y, \\ & \forall \mathbf{x}^{(0)} \in \mathbf{D}_{val}. \end{aligned} \quad (11)$$

The corresponding constraints to Equation (9) and Equation (10) in the above optimization problem are slightly different from their original forms presented previously. Let us consider Equation (9), for instance. Here, for each neuron  $i$ , if the neuron has been originally active, we introduce  $\tilde{\mathbf{W}}_{i,:}^{(l)} \mathbf{x}^{(l-1)} + \tilde{b}_i^{(l)} \geq 0$  and  $\tilde{x}_i^{(l)} = \tilde{\mathbf{W}}_{i,:}^{(l)} \mathbf{x}^{(l-1)} + \tilde{b}_i^{(l)}$  constraints; otherwise, we introduce  $\tilde{\mathbf{W}}_{i,:}^{(l)} \mathbf{x}^{(l-1)} + \tilde{b}_i^{(l)} \leq 0$  and  $\tilde{x}_i^{(l)} = 0$  constraints.

Equation (11) has a hyperparameter  $\epsilon$  that can take a wide range of values. If  $\epsilon = 0$ , the value of each neuron is not allowed to change after optimization, i.e.,  $\tilde{\mathbf{x}}^{(l)} = \mathbf{x}^{(l)}$ . If  $\epsilon > 0$ , then  $\tilde{\mathbf{x}}^{(l)}$  can be different from  $\mathbf{x}^{(l)}$  and the optimization has more freedom to find more sparse neural networks.

### F. End-to-End Optimization Problem

The optimization problem in Equation (11) only targets a single layer  $l$ . Here, we propose an end-to-end process to generate VNNs for the entire neural network iteratively. We initiate the process with an already-trained model along with a validation set. The process proceeds layer-by-layer to obtain sparse weights and biases for the neural network model. To find a more verification-friendly model within our framework, we start from the first hidden layer,  $l = 1$ , and run the optimization problem in Equation (11) to find the sparse matrix of weights and vector biases such that the outcome of the classification on the validation set remains unchanged. Then, the weights and biases of the first hidden layer,  $\tilde{\mathbf{W}}^{(1)}$  and  $\tilde{\mathbf{b}}^{(1)}$ , remain unaltered, while the optimization is performed solely on the second hidden layer to detect the sparse  $\tilde{\mathbf{W}}^{(2)}$  and  $\tilde{\mathbf{b}}^{(2)}$ . This process continues until the final layer of the neural network.

## III. EVALUATION

In this section, we assess the effectiveness of our proposed framework by evaluating its performance on different well-established datasets. Our framework is implemented using the Gurobi solver [19]. The experiments are conducted using a MacBook Pro with an 8-core CPU and 32 GB of RAM.

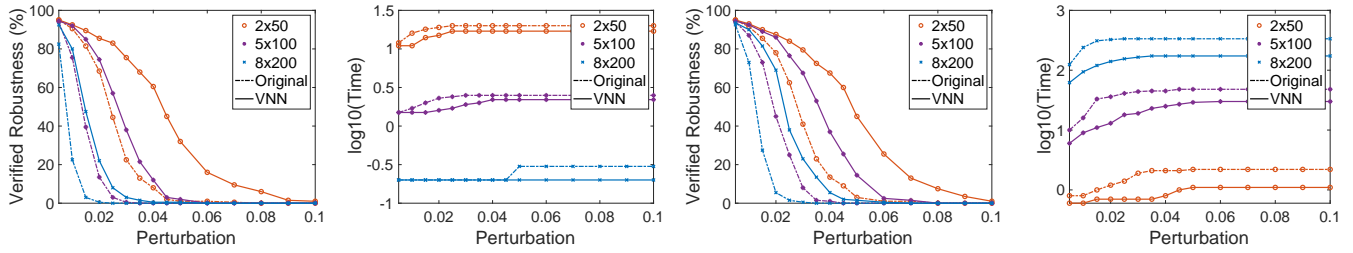
### A. Datasets

We consider three public datasets for evaluation of VNNs in this work, namely, the MNIST dataset [12] and two datasets from safety-critical medical applications. The first one is about epileptic seizure detection based on the CHB-MIT Scalp EEG database [13] and the second one concerns cardiac arrhythmia detection based on the MIT-BIH Arrhythmia database [14].

**MNIST image dataset [12]** is composed of grayscale handwritten digits such that each digit is represented by a  $28 \times 28$  pixel image. Similar to [8], we consider the first 400 images of the test set and equally split MNIST into a validation set and a test set for the refinement/optimization and evaluation of the networks.

**CHB-MIT dataset [13]** comprises 23 individuals diagnosed with epileptic seizures, consisting of 5 males and 17 females in the age range of 1.5 to 22 years. This dataset is recorded in the international 10-20 system of EEG electrode positions and nomenclature. We utilize two electrode pairs, namely F7-T7 and F8-T8, which are frequently employed in seizure detection research [20]. The recordings were performed at a sampling frequency of 256 Hz and each sample has a 4-second duration. For each patient, we consider 60%, 20%, and 20% of the dataset for the training, validation, and test sets, respectively. The set sizes vary among patients, and each patient's entire dataset consists of 44 to 1009 samples, with an average of 252 samples.

**MIT-BIH dataset [14]** contains 48 records of 2-channel ECG signals, which have been digitized with a sampling rate of 360 Hz. The dataset includes 25 male and 22 female subjects aged 23 to 89 years. However, 65% of the total



(a) Verified robustness on MNIST using ERAN (b) Average processing time on MNIST using ERAN (c) Verified robustness on MNIST using SafeDeep (d) Average processing time on MNIST using SafeDeep

Fig. 1: Verified robustness and average processing time, in base 10 logarithm, of the MNIST dataset w.r.t. different values of perturbations for original models and VNNs using ERAN and SafeDeep.

subjects were found to have only one class of heartbeats. To be able to formulate a classification problem, we select the 14 subjects with at least two distinct types of heartbeats. Similar to the CHB-MIT dataset, each model is trained using a training set, optimized with a validation set, and evaluated using a test set. The training set includes 75% of the entire dataset. The remaining 25% are equally partitioned among the test set and the validation set. The size of the datasets may differ among the patients and each patient’s entire set consists of 400 to 1800 samples, with an average of 957 samples.

### B. Neural Network Models

We consider Fully-connected Neural Networks (FNNs) and Convolutional Neural Networks (CNNs) to investigate the performance of our proposed framework.

**FNNs.** We adopt FNNs trained by [8] on MNIST to explore the performance of our framework. We examined six FNNs with different numbers of neurons, where each dense layer is followed by a ReLU activation function. The models have  $2 \times 50$ ,  $2 \times 100$ ,  $5 \times 100$ ,  $5 \times 200$ ,  $8 \times 100$ , and  $8 \times 200$  hidden layers. The input and output layers have 784 and 10 neurons, respectively.

**CNNs.** We train CNNs on CHB-MIT and MIT-BIH datasets to study the compatibility of our framework with CNNs. For the CHB-MIT dataset, we generated 23 personalized neural networks, one for each patient. Each model consists of three hidden layers, including two convolutional layers with 3 and 5 filters and kernel sizes of 100 and 200, respectively, as well as a dense layer with 40 neurons. The input layer has 2048 neurons. For the MIT-BIH dataset, we have 14 individual neural networks, each with an input layer of 320 neurons, a convolutional layer with a kernel size of 64 and 3 filters, and a dense layer with 40 neurons. The output layer of all CNNs has two output neurons to classify the input into negative (non-seizure/normal) or positive (seizure/arrhythmia) classes. The average accuracy of the neural networks for CHB-MIT and MIT-BIH datasets on the test set is  $85.7\% \pm 14.8\%$  and  $92.2\% \pm 9.1\%$ , respectively.

### C. Robustness Properties

The robustness property is formulated in terms of the  $L_\infty$  norm and is parameterized by a constant  $\delta$ . The adversarial region includes all perturbed inputs such that each input neuron has a maximum distance of  $\delta$  from the corresponding neuron’s value in the original input. The range of perturbation is considered differently for different datasets, as it depends on the robustness of each neural network w.r.t. its structure and application. The maximum studied perturbations for MNIST, CHB-MIT, and MIT-BIH are 0.1, 0.01, and 0.2, respectively.

### D. Verification Frameworks

We consider ERAN [8] and SafeDeep [11] to assess the effectiveness of our proposed framework in this paper. ERAN and SafeDeep are over-approximation-based frameworks designed to verify the robustness of DNNs. ERAN, or more specifically DeepPoly, works based on the principles of abstract interpretation. SafeDeep, on the other hand, works based on incremental refinement of convex/linear approximations.

### E. Results and Analysis

In this section, we evaluate our proposed framework in terms of provability of robustness. We shall first evaluate the proposed VNN models considering the MNIST dataset.

**MNIST.** Let us now evaluate the VNNs generated by our proposed framework against pre-trained original models. Tables I and II show the robustness and execution time of FNNs evaluated by ERAN and SafeDeep. We select five different perturbation values to cover a wide range of perturbations and evaluated the test set for the neural networks. Based on the results shown in Table I, the number of samples for which robustness could be established for the VNNs is significantly larger than that of the original DNNs. Moreover, as the perturbation increases, the difference in the number of verified samples becomes even more significant. We select three neural networks with  $2 \times 50$ ,  $5 \times 100$ , and  $8 \times 200$  hidden layers as representatives of small, medium, and large neural network models, respectively, in Figure 1. Based on the results in Figures 1a and 1c, we observe that the accuracy of all VNNs is almost the same as their corresponding original models. In addition, the verification tools consistently establish

TABLE I: Verified robustness (%) of original models and VNNs ( $\epsilon = 0$ ) on the MNIST dataset for six FNNs with different structures using ERAN and SafeDeep. VNNs are optimized models that are more verification friendly than the original models.

Model	ERAN [8]										SafeDeep [11]									
	$\delta = 0.01$		$\delta = 0.02$		$\delta = 0.03$		$\delta = 0.05$		$\delta = 0.07$		$\delta = 0.01$		$\delta = 0.02$		$\delta = 0.03$		$\delta = 0.05$		$\delta = 0.07$	
	Org	VNN	Org	VNN	Org	VNN	Org	VNN	Org	VNN	Org	VNN	Org	VNN	Org	VNN	Org	VNN	Org	VNN
$2 \times 50$	90.5	92.5	68.5	85.5	22.5	75.5	1	32	0.5	9.5	91.5	93	78	87.5	41	79.5	3	45	1	13
$2 \times 100$	85	92.5	33.5	85	3.5	70	0	16.5	0	2	90.5	92.5	67.5	86.5	15.5	77.5	0	33.5	0	7
$5 \times 100$	75.5	92	13.5	74.5	0.5	38	0	2	0	0	87	92.5	45	86	8	67.5	0	14.5	0	1.5
$5 \times 200$	27	84	0.5	29.5	0	4.5	0	0	0	0	76	90	7	73	0	27	0	1	0	0
$8 \times 100$	67	85	17.5	60.5	0.5	28	0	3.5	0	0	84	90	40	79	11.5	56	0	16.5	0	1.5
$8 \times 200$	22.5	80	0.5	22	0	3	0	0.5	0	0	73	90	5.5	69	0.5	23	0	1.5	0	0

TABLE II: Average processing time (s) of original models and VNNs ( $\epsilon = 0$ ) on the MNIST dataset for six FNNs with different structures using ERAN and SafeDeep. VNNs are optimized verification-friendly models for which the robustness verification is more efficient in terms of time, when compared against the original neural networks.

Model	ERAN [8]										SafeDeep [11]									
	$\delta = 0.01$		$\delta = 0.02$		$\delta = 0.03$		$\delta = 0.05$		$\delta = 0.07$		$\delta = 0.01$		$\delta = 0.02$		$\delta = 0.03$		$\delta = 0.05$		$\delta = 0.07$	
	Org	VNN																		
$2 \times 50$	0.2	0.2	0.2	0.2	0.2	0.2	0.3	0.2	0.3	0.2	0.8	0.6	1.2	0.7	1.9	0.7	2.2	1.1	2.2	1.1
$2 \times 100$	0.5	0.4	0.6	0.5	0.7	0.5	0.8	0.6	0.8	0.7	2.7	1.7	7.6	1.9	7.6	2.6	10	4.2	10	4.2
$5 \times 100$	1.7	1.5	2.3	1.6	2.5	1.9	2.5	2.2	2.5	2.2	16	9	36	13	44	19	48	29	48	30
$5 \times 200$	8	6	9	7	9	8	9	8	9	8	106	35	180	68	180	88	180	94	180	94
$8 \times 100$	3	3	4	3	5	4	5	4	5	5	46	21	93	31	111	51	123	60	123	87
$8 \times 200$	16	11	19	15	20	17	20	17	20	17	240	94	325	140	335	165	335	173	335	173

robustness for more samples and for larger perturbations for VNNs. Moreover, Figures 1b and 1d show that the average processing time for each sample increases when considering larger perturbations. Indeed, the execution time of VNNs is up to two times less than their corresponding original models. This happens due to the fewer number of over-approximated neurons that is caused by sparsening the weights and biases of the neural network. Note that in Figures 1b and 1d the y-axis is the logarithm of the average time period.

**Hyperparameter.** Next, we investigate how changing the hyperparameter  $\epsilon$  impacts robustness on three FNNs with different structures based on the MNIST dataset. We show in Figure 2 the results obtained using SafeDeep. The key idea is to relax the constraints, which leads to an optimization problem with a larger solution space, to obtain a sparser solution in the optimization problem with fewer non-zero neurons. For example, when  $\epsilon = 0.1$ , the value of each neuron  $\tilde{x}_i^{(l)}$  can change in the range of  $[0.9x_i^{(l)}, 1.1x_i^{(l)}]$ , and this freedom of choices allows for sparser models that are easier to handle by the over-approximation-based verification frameworks. However, a too small validation set, in comparison to the size of the model, can lead to a decrease in the model’s prediction performance. Figure 2a displays the verification results obtained for the original and VNN models for a small network with two fully-connected layers each with 50 hidden neurons. As the neural network is small in comparison to the size of the validation set, which contains 200 samples, the accuracy of optimized models does not drop dramatically when  $\epsilon$  increases up to 0.5, while the robustness increases up to 10% for large perturbations. On the other hand, Figures 2b

and 2c illustrate a significant decrease in accuracy (the y-axis captures accuracy in the absence of a perturbation) when  $\epsilon$  increases. This is due to the small size of the validation set in relation to the sizes of the networks. Based on Figure 2b, when  $\epsilon = 0.2$ , the medium size neural network with five layers each containing 100 neurons has a minor drop in its accuracy, while performance improved in terms of robustness. Figure 2c shows the results of the largest models we explored in this paper that show an explicit trade-off between accuracy and robustness. When  $\epsilon = 0$  or  $\epsilon = 0.1$ , the accuracy is above 90% and the model is more robust against small values of perturbation, while with  $\epsilon = 0.2$ , the accuracy slightly decreases. However, if we consider  $\epsilon \geq 0.3$ , the accuracy of the network decreases dramatically. To avoid this degradation, it is possible to increase the size of the validation set to maintain the prediction performance at the required level.

**Number of Optimized Layers.** Our proposed framework optimizes the entire neural network model iteratively and layer by layer. The number of optimized layers is, therefore, another parameter that can affect the performance of our proposed framework. Figure 3 shows the robustness results for a VNN with  $8 \times 200$  hidden layers and  $\epsilon = 0.2$  using SafeDeep. The x-axis shows the number of layers that are optimized using our framework, e.g., 3 means the first 3 hidden layers are optimized in the corresponding model. Each curve shows the verification results obtained by SafeDeep w.r.t. a specific value of perturbation  $\delta$  to be able to compare the effectiveness of increasing the number of optimized layers in a neural network. Figure 3 demonstrates that as the number of optimized layers increases, shown on the x-axis, the number of

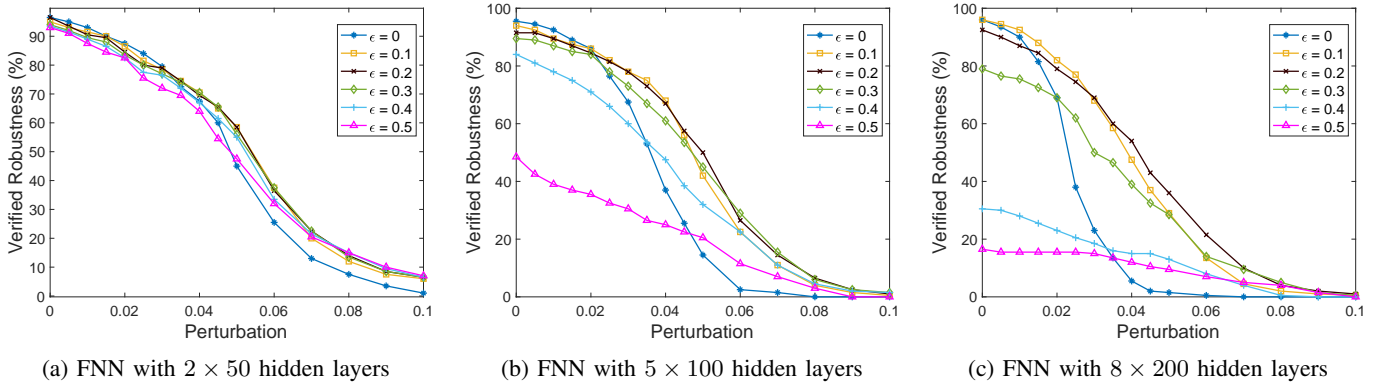


Fig. 2: The effectiveness of  $\epsilon$  for different neural network structures. Generally, there is a trade off between the value of  $\epsilon$ , the accuracy of the model, and its robustness. Moreover, the proportion of the validation set size and the number of hidden neurons affects the performance of optimized models.

verified cases increases. The reason behind this phenomenon is that increasing the number of optimized layers leads to decreasing the over-approximation of each layer and therefore the neural network becomes more verification friendly.

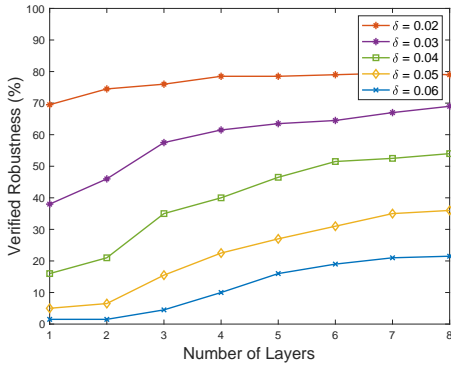


Fig. 3: Increasing the number of optimized layers in an FNN with  $8 \times 200$  hidden layers results in increasing the number of samples whose robustness is verified.

**Comparison with Straightforward Pruning.** Let us now compare our proposed technique against a baseline model obtained by pruning the weights/biases below a threshold to zero [21]. To ensure a fair comparison, we ensure that the number of zero weights/biases are equal for the baseline models and VNNs. Figure 4 shows the number of samples for which the robustness could be established/verified for the baseline/pruned models and VNNs for several neural networks with different sizes. These results demonstrate that while the baseline models and VNNs have similar accuracy for smaller neural networks, there is a major degradation in the accuracy of the baseline models for larger neural networks (24.5% for baseline/pruned model of model  $8 \times 200$  with perturbation 0).

Next, we evaluate our proposed framework in the context of two safety-critical medical applications, namely, epileptic

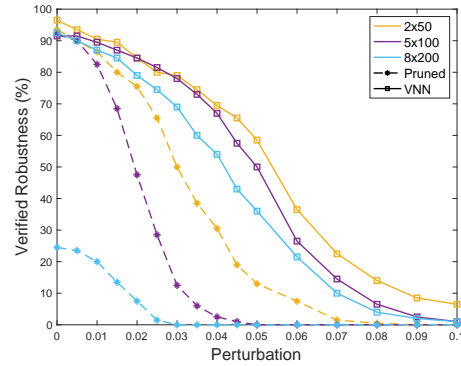


Fig. 4: Verified robustness of VNNs and baseline/pruned models with straightforward pruning.

seizure detection and cardiac arrhythmia detection, to demonstrate its relevance.

**CHB-MIT.** Let us now investigate the effectiveness of our proposed framework based on the CHB-MIT dataset. Figures 5a and 5b show the verified robustness curves using ERAN and SafeDeep, where perturbation  $\delta$  is in the range of  $[0.0001, 0.01]$ . Here, the curves demonstrate the average number of samples for which robustness is validated and the shaded areas represent the variance w.r.t. the patients. The verified robustness of three different models is evaluated on all the patients in CHB-MIT dataset to investigate their behavior for different perturbations. The accuracy ( $\mu \pm \sigma^2$ ) of the original models and VNNs on the test sets are  $85.7\% \pm 3.8\%$  and  $82.5\% \pm 4.2\%$ , respectively, while the VNNs are substantially more verification friendly. Here, we also look into a baseline model that is called a pruned model [21]. A pruned model is a model obtained from an original model by setting the 10% smallest weights to zero. Higher rates significantly decrease the accuracy of the pruned models. Although model pruning using a fixed threshold improves robustness verification exploring by established over-approximation-based methods, it

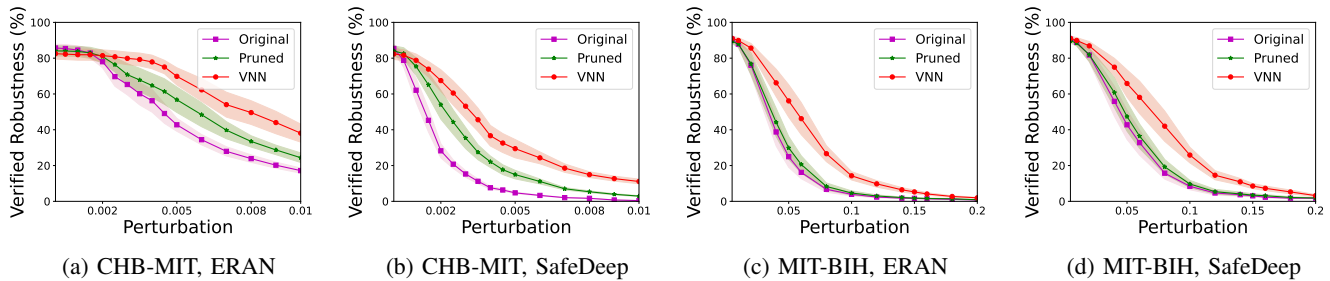


Fig. 5: Mean and variance of verified robustness cases for the CHB-MIT and MIT-BIH datasets. Baseline/pruned models are generated using a threshold that forces small weights to become zero, and VNNs are generated using our proposed framework.

is not as effective as our proposed optimization framework. Indeed, using a fixed threshold to disregard weights not only does not minimize the number of non-zero elements but also ignores the model accuracy. Our proposed framework, on the other hand, actively looks for weights that maintain accuracy while forcing as many weights and biases as possible to become zero. For the CHB-MIT dataset, the accuracy of the pruned models on the test sets is  $84.1\% \pm 4.1\%$ , which is only slightly higher than our optimized models, but our framework is up to one order of magnitude more verification friendly. This slight difference in accuracy is because VNNs are approximately 40% more sparse. However, the accuracy of the baseline models drops to  $68.4\% \pm 4.3\%$ , if we enforce the baseline models to have similar sparsity as our VNNs. In summary, our framework generates VNNs that have up to 9 and 21 times more verified robustness using ERAN and SafeDeep, respectively.

**MIT-BIH.** Next, we investigate the effectiveness of our framework considering the MIT-BIH dataset using ERAN and SafeDeep. As shown in Figures 5c and 5d, VNNs generated by our proposed framework verify the robustness of more samples, and their performance w.r.t. robustness verification is better for higher values of perturbations. Figures 5c and 5d show the verified robustness of original models, baseline/pruned models, and VNNs, with accuracy  $91.5\% \pm 3.1\%$ ,  $90.7\% \pm 3.4\%$ , and  $92.0\% \pm 3.0\%$ , respectively. The experiments show that our proposed framework generates VNNs that have up to 34 and 30 times more verified robustness using ERAN and SafeDeep, respectively.

#### IV. RELATED WORK

Neural networks are known for their vulnerability to adversarial examples [22]. Adversarial examples are obtained by slight modification of correctly classified inputs, essentially leading to inputs that are misclassified by the network despite their extreme similarity to the original correctly classified inputs. Below, we review several studies aiming at improving the scalability of robustness verification of neural networks against adversarial examples.

One prominent research direction in this domain aims at enhancing the scalability of verification techniques for establishing robustness properties for DNNs. Here, the state-of-

the-art techniques for verification robustness of DNNs can be categorized as either precise [6, 7, 5] or based on over-approximation [8, 23, 24, 11]. The exact techniques face fundamental challenges in scalability due to their exhaustive exploration of all potential behaviors, often leading to exponential complexity [5]. On the other hand, the over-approximation-based approaches prioritize scalability over precision, but still limited by the inherent trade-off between scalability and precision.

Other studies have sought to establish links between model robustness and the architecture of deep neural networks. Lin et al. [25] demonstrated that binarization enhances robustness by keeping the noise magnitude small. Another study revealed that quantized neural networks exhibit greater scalability, but their accuracy is compromised as they disregard floating-point values [26]. In [27], it was also shown that robustness against adversarial attacks improves if redundant neurons are eliminated. Guidotti et al. [21] utilized network pruning to reduce the size of neural networks by eliminating non-crucial portions that do not significantly impact their performance. However, the proposed technique is mainly applicable to small-scale neural networks (with 112 hidden neurons) and does not scale to larger neural networks (e.g., with 224 hidden neurons).

#### V. CONCLUSIONS

The state-of-the-art verification tools currently face major challenges in terms of scalability. In this paper, we presented an optimization framework to generate a new class of DNNs, referred to as VNNs, that are amenable to verification, or simply verification friendly. VNNs allow more efficiency, in terms of time, and/or more verified samples, while maintaining on-par prediction performance with their DNN counterparts. To obtain VNNs, we formulate an optimization problem on pre-trained models to generate VNNs while maintaining on-par prediction performance. Our experimental evaluation based on MNIST, CHB-MIT, and MIT-BIH datasets demonstrates that the robustness of our proposed VNNs can be established substantially more often and in a more time-efficient manner than their DNN counterparts, without any major loss in terms of prediction performance.

## REFERENCES

- [1] Seyed-Mohsen Moosavi-Dezfooli, Alhussein Fawzi, and Pascal Frossard. Deepfool: a simple and accurate method to fool deep neural networks. In *Computer Vision and Pattern Recognition (CVPR)*, pages 2574–2582. IEEE, 2016.
- [2] Alexey Kurakin, Ian J Goodfellow, and Samy Bengio. Adversarial examples in the physical world. In *Artificial intelligence safety and security*, pages 99–112. Chapman and Hall/CRC, 2018.
- [3] Hongshuo Liang, Erlu He, Yangyang Zhao, Zhe Jia, and Hao Li. Adversarial attack and defense: A survey. *Electronics*, 11(8):1283, 2022.
- [4] Xiaowei Huang, Daniel Kroening, Wenjie Ruan, James Sharp, Youcheng Sun, Emese Thamo, Min Wu, and Xiping Yi. A survey of safety and trustworthiness of deep neural networks. *arXiv preprint arXiv:1812.08342*, 2018.
- [5] Guy Katz, Clark Barrett, David L Dill, Kyle Julian, and Mykel J Kochenderfer. Reluplex: An efficient smt solver for verifying deep neural networks. In *Computer-Aided Verification (CAV)*, pages 97–117. Springer, 2017.
- [6] Vincent Tjeng, Kai Xiao, and Russ Tedrake. Evaluating robustness of neural networks with mixed integer programming, 2017.
- [7] Xiaowei Huang, Marta Kwiatkowska, Sen Wang, and Min Wu. Safety verification of deep neural networks. In *Computer-Aided Verification (CAV)*, pages 3–29. Springer, 2017.
- [8] Gagandeep Singh, Timon Gehr, Markus Püschel, and Martin Vechev. An abstract domain for certifying neural networks. *Proceedings of the ACM on Programming Languages (PACMPL)*, 3:1–30, 2019.
- [9] Guy Katz, Derek A Huang, Duligur Ibeling, Kyle Julian, Christopher Lazarus, Rachel Lim, Parth Shah, Shantanu Thakoor, Haoze Wu, Aleksandar Zeljić, et al. The marabou framework for verification and analysis of deep neural networks. In *Computer-Aided Verification (CAV)*, pages 443–452. Springer, 2019.
- [10] Gagandeep Singh, Rupanshu Ganvir, Markus Püschel, and Martin Vechev. Beyond the single neuron convex barrier for neural network certification. *Advances in Neural Information Processing Systems*, 32, 2019.
- [11] Anahita Baninajjar, Kamran Hosseini, Ahmed Rezine, and Amir Aminifar. Safedeep: A scalable robustness verification framework for deep neural networks. In *ICASSP 2023-2023 IEEE International Conference on Acoustics, Speech and Signal Processing (ICASSP)*, pages 1–5. IEEE, 2023.
- [12] Yann LeCun. The mnist database of handwritten digits. <http://yann.lecun.com/exdb/mnist/>, 1998.
- [13] Ali Shoeb. CHB-MIT Scalp EEG Database, 2010.
- [14] Ary L Goldberger, Luis AN Amaral, Leon Glass, Jeffrey M Hausdorff, Plamen Ch Ivanov, Roger G Mark, Joseph E Mietus, George B Moody, Chung-Kang Peng, and H Eugene Stanley. MIT-BIH Arrhythmia Database, 2000.
- [15] Rosemary J Panelli. Sudep: a global perspective. *Epilepsy & Behavior*, 103:106417, 2020.
- [16] Roland X Stroobandt, Mattias F Duytschaever, Teresa Strisciuglio, Frederic E Van Heuverswyn, Liesbeth Timmers, Jan De Pooter, Sébastien Knecht, Yves R Vandekerckhove, Andreas Kucher, and Rene H Tavernier. Failure to detect life-threatening arrhythmias in icds using single-chamber detection criteria. *Pacing and Clinical Electrophysiology*, 42(6):583–594, 2019.
- [17] Yu-Liang Chou, Catarina Moreira, Peter Bruza, Chun Ouyang, and Joaquim Jorge. Counterfactuals and causability in explainable artificial intelligence: Theory, algorithms, and applications. *Information Fusion*, 81:59–83, 2022.
- [18] Ron Zass and Amnon Shashua. Nonnegative sparse pca. *Advances in neural information processing systems*, 19, 2006.
- [19] Gurobi Optimization, LLC. Gurobi Optimizer Reference Manual, 2023.
- [20] Dionisije Sopic, Amir Aminifar, and David Atienza. e-glass: A wearable system for real-time detection of epileptic seizures. In *2018 IEEE International Symposium on Circuits and Systems (ISCAS)*, pages 1–5, 2018.
- [21] Dario Guidotti, Francesco Leofante, Luca Pulina, and Armando Tacchella. Verification of neural networks: Enhancing scalability through pruning. *arXiv preprint arXiv:2003.07636*, 2020.
- [22] Christian Szegedy, Wojciech Zaremba, Ilya Sutskever, Joan Bruna, Dumitru Erhan, Ian Goodfellow, and Rob Fergus. Intriguing properties of neural networks. *arXiv preprint arXiv:1312.6199*, 2013.
- [23] Lily Weng, Huan Zhang, Hongge Chen, Zhao Song, Cho-Jui Hsieh, Luca Daniel, Duane Boning, and Inderjit Dhillon. Towards fast computation of certified robustness for relu networks. In *International Conference on Machine Learning (ICML)*, pages 5276–5285. PMLR, 2018.
- [24] Rudy R Bunel, Ilker Turkaslan, Philip Torr, Pushmeet Kohli, and Pawan K Mudigonda. A unified view of piecewise linear neural network verification. *Advances in Neural Information Processing Systems*, 31, 2018.
- [25] Ji Lin, Chuang Gan, and Song Han. Defensive quantization: When efficiency meets robustness. *arXiv preprint arXiv:1904.08444*, 2019.
- [26] Thomas A Henzinger, Mathias Lechner, and Dorde Zikelic. Scalable verification of quantized neural networks. In *Proceedings of the AAAI Conference on Artificial Intelligence*, volume 35, pages 3787–3795, 2021.
- [27] Sietsma and Dow. Neural net pruning-why and how. In *IEEE 1988 international conference on neural networks*, pages 325–333. IEEE, 1988.